Searches for Gravitational Waves from Known Pulsars at Two Harmonics in the Second and Third LIGO-Virgo Observing Runs

(Abbott et al 2022 ApJ 935 1)

Paritosh Verma
(On behalf of LIGO-Virgo-KAGRA collaboration)
Narodowe Centrum Badań Jądrowych (NCBJ)
Otwock, Poland

The 8th Conference of the Polish Society on Relativity
September 19, 2022

Pulsars

- Pulsars are a special kind of neutron stars.
- They emit a beam of radiation which we observe as a periodic pulse as the beam sweeps over us once per rotation.

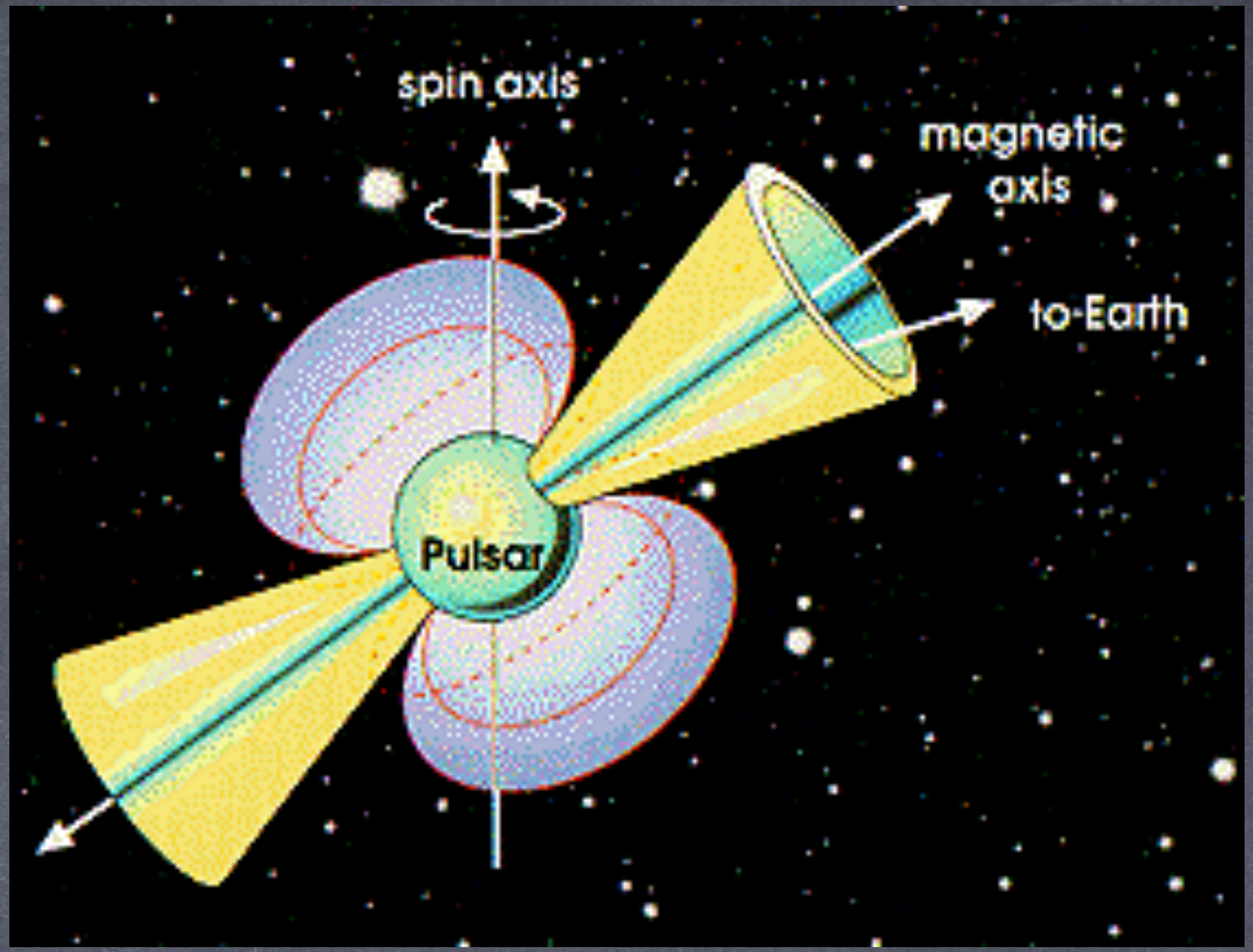

Courtesy: Imagine the Universe NASA/GSFC.

Particles accelerated along strong magnetic field lines produce beam of radiation. If magnetic field is not aligned the spin axis, this gives lighthouse effect.

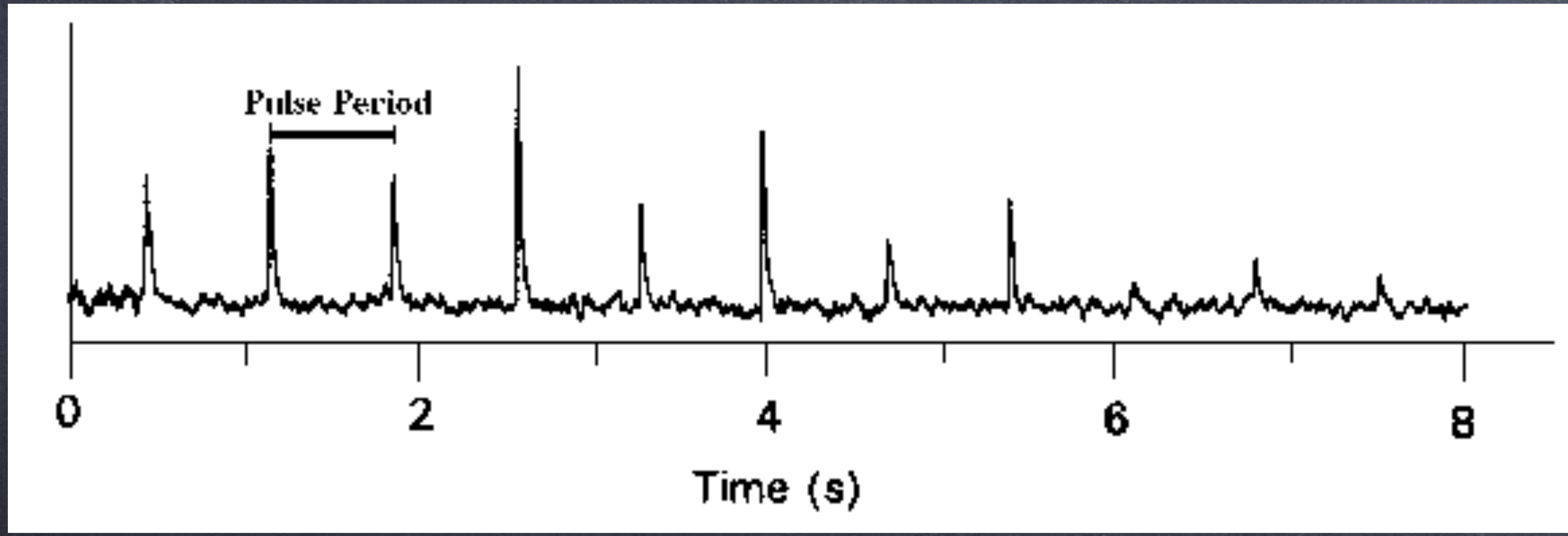

Courtesy: Manchester, R.N and Taylor, J.H., Pulsars, Freeman, 1977.

- 1934: Walter Baade and Fritz Zwicky predicted the existence of NS
- 1967: First pulsar was discovered by Jocelyn Bell and Anthony Hewish.

Pulsars (contd.)

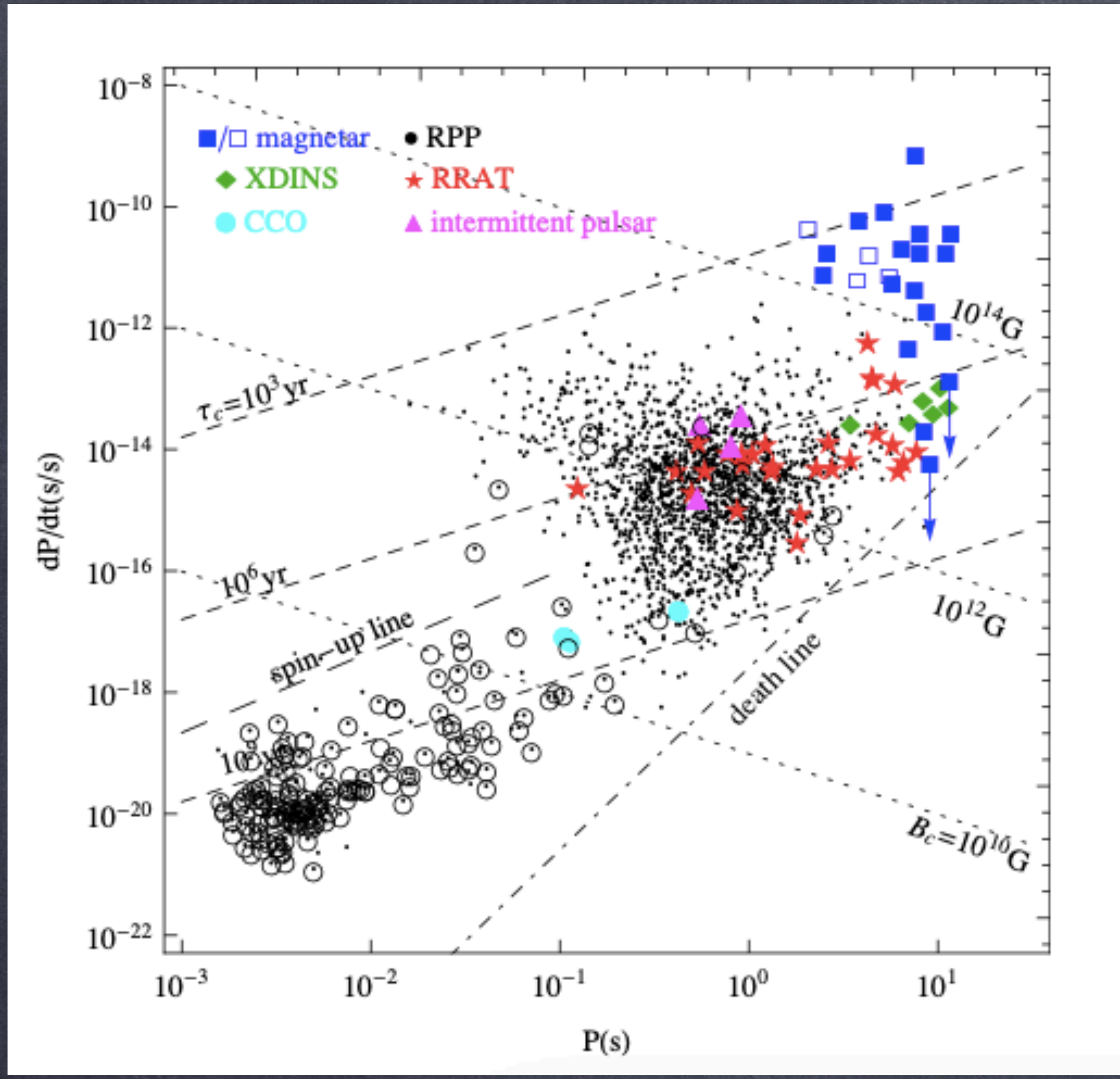

Courtesy: arxiv 1508.03115

Estimated magnetic field: $B = 3.2 \times 10^{19} \sqrt{P\dot{P}} \;\; G$

Standard pulsar: $B \approx 10^{12} \;\; G$

Accreting pulsar: $B \approx 10^{8} \;\; G$

Magnetar: $B \approx 10^{15} \;\; G$

A rough estimate of pulsar's age: $\tau_c = \dfrac{P}{2\dot{P}}$

- Young and strongly magnetized pulsars: Top right hand corner

- Old and weakly magnetized pulsars: Bottom left

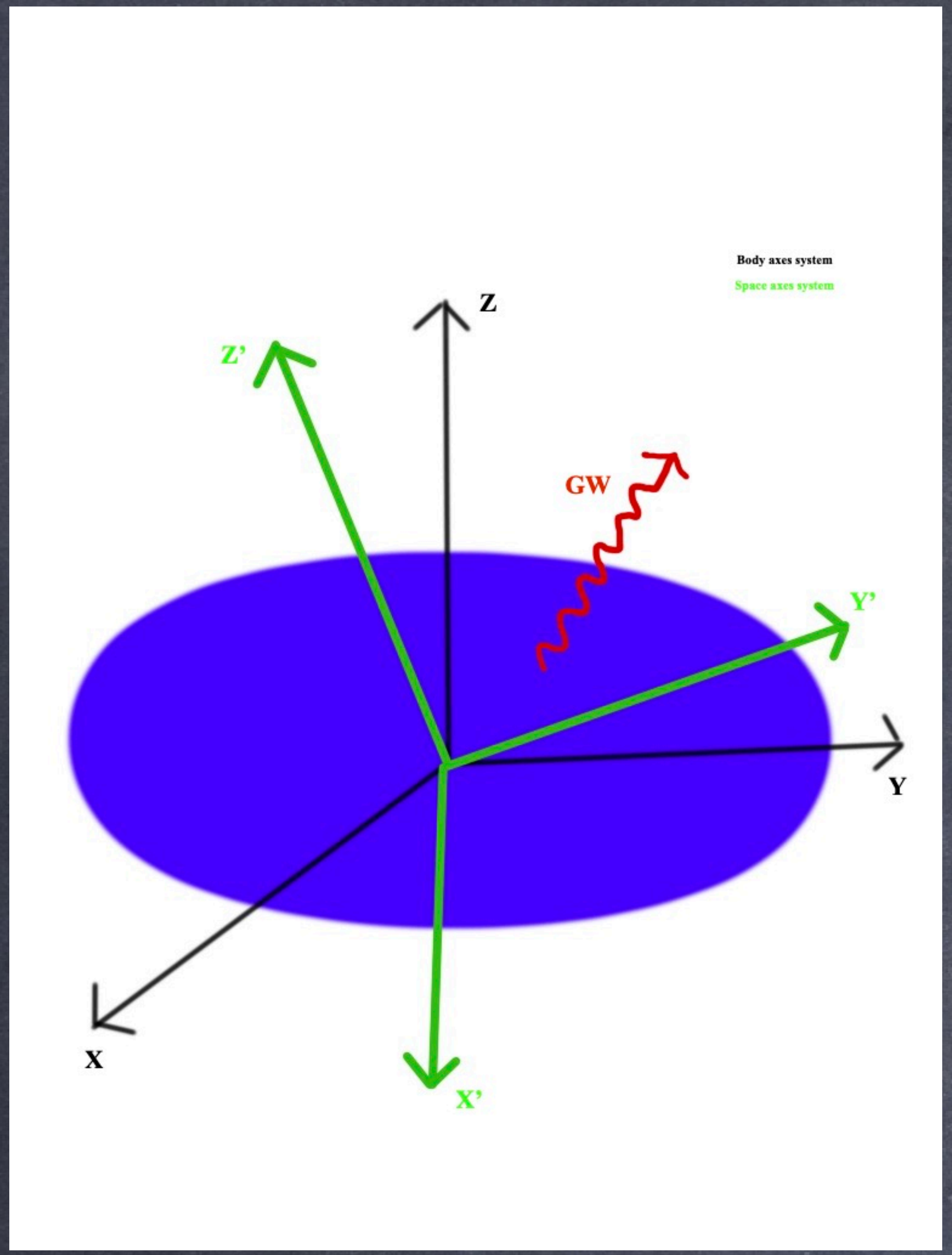

Dual Harmonics

$$\vec{L} = \begin{bmatrix} I_{xx} & I_{xy} & I_{xz} \\ I_{yx} & I_{yy} & I_{yz} \\ I_{zx} & I_{zy} & I_{zz} \end{bmatrix} \begin{bmatrix} 0 \\ 0 \\ 2\pi f_{\rm rot} \end{bmatrix}$$

$$L_x = 2\pi f_{\rm rot} I_{xz}$$
$$L_y = 2\pi f_{\rm rot} I_{yz}$$
$$L_z = 2\pi f_{\rm rot} I_{zz}$$

The angular velocity in the Z'-direction produces angular momentum in all three directions. In this case;

$f_{\rm GW} = f_{\rm rot}\ (l = 2,\ m = 1)$ and $f_{\rm GW} = 2f_{\rm rot}\ (l = 2,\ m = 2)$

$$h_{21} = -\frac{C_{21}}{2}\left[F_+^D(\alpha,\delta,\psi;t)\sin\iota\cos\iota\cos\left(\Phi(t)+\Phi_{21}^C\right) + F_\times^D(\alpha,\delta,\psi;t)\sin\iota\sin\left(\Phi(t)+\Phi_{21}^C\right)\right]$$

$$h_{22} = -C_{22}\left[F_+^D(\alpha,\delta,\psi;t)(1+\cos^2\iota)\cos\left(2\Phi(t)+\Phi_{22}^C\right) + 2F_\times^D(\alpha,\delta,\psi;t)\cos\iota\sin\left(2\Phi(t)+\Phi_{22}^C\right)\right]$$

C_{21} and C_{22} : dimensionless constants

α and δ : right ascension and declination of the source

ι and ψ : describe the orientation of the source's spin axis with respect to the observer in terms of inclination and polarization

Φ_{21}^C and Φ_{22}^C : phase angles at a defined epoch

$\Phi(t)$: rotational phase of the source

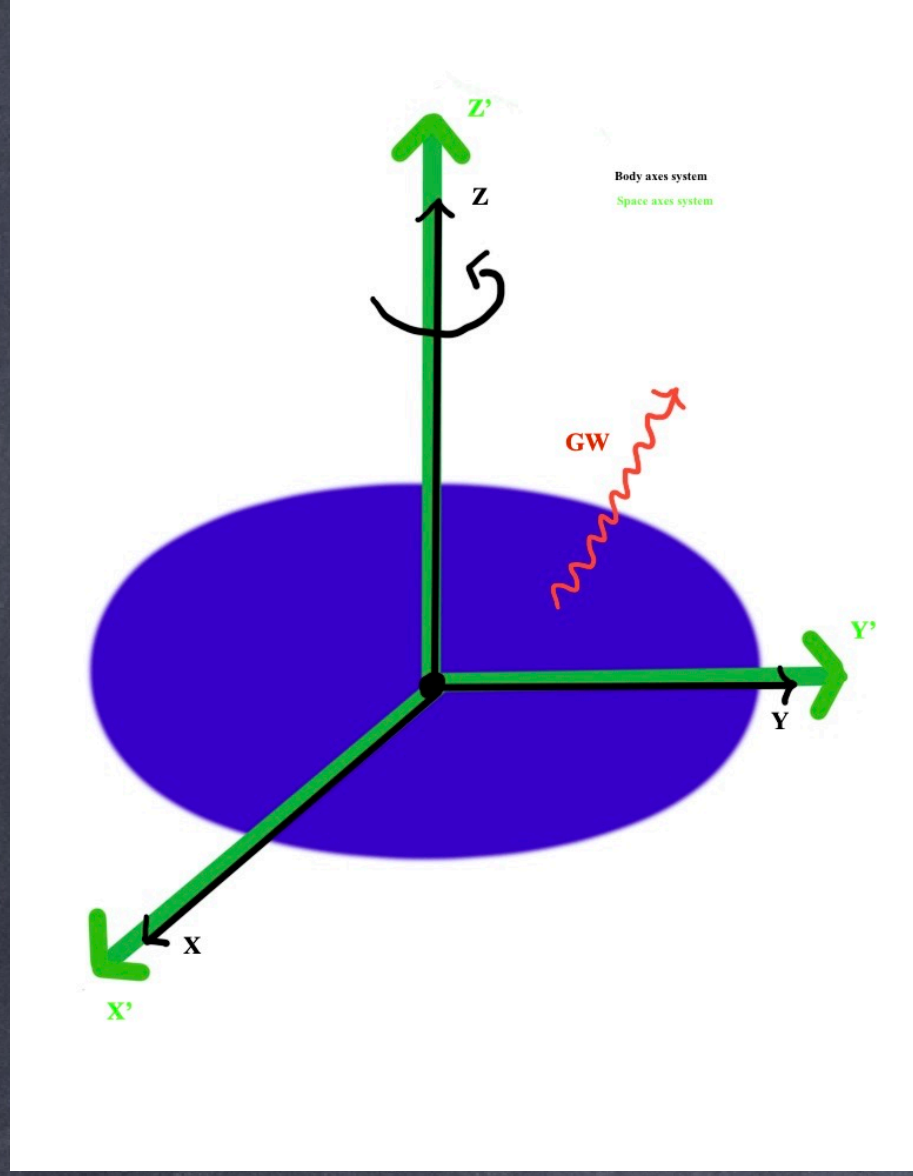

Single Harmonic

$$\vec{L} = \begin{bmatrix} I_{xx} & 0 & 0 \\ 0 & I_{yy} & 0 \\ 0 & 0 & I_{zz} \end{bmatrix} \begin{bmatrix} 0 \\ 0 \\ 2\pi f_{\mathrm{rot}} \end{bmatrix}$$

$$L_x = L_y = 0$$

$$L_z = 2\pi f_{\mathrm{rot}} I_{zz}$$

The angular velocity in the Z'-direction produces angular momentum only in the Z'-direction. In this case; $f_{\mathrm{GW}} = 2f_{\mathrm{rot}} \quad (l = 2,\, m = 2)$

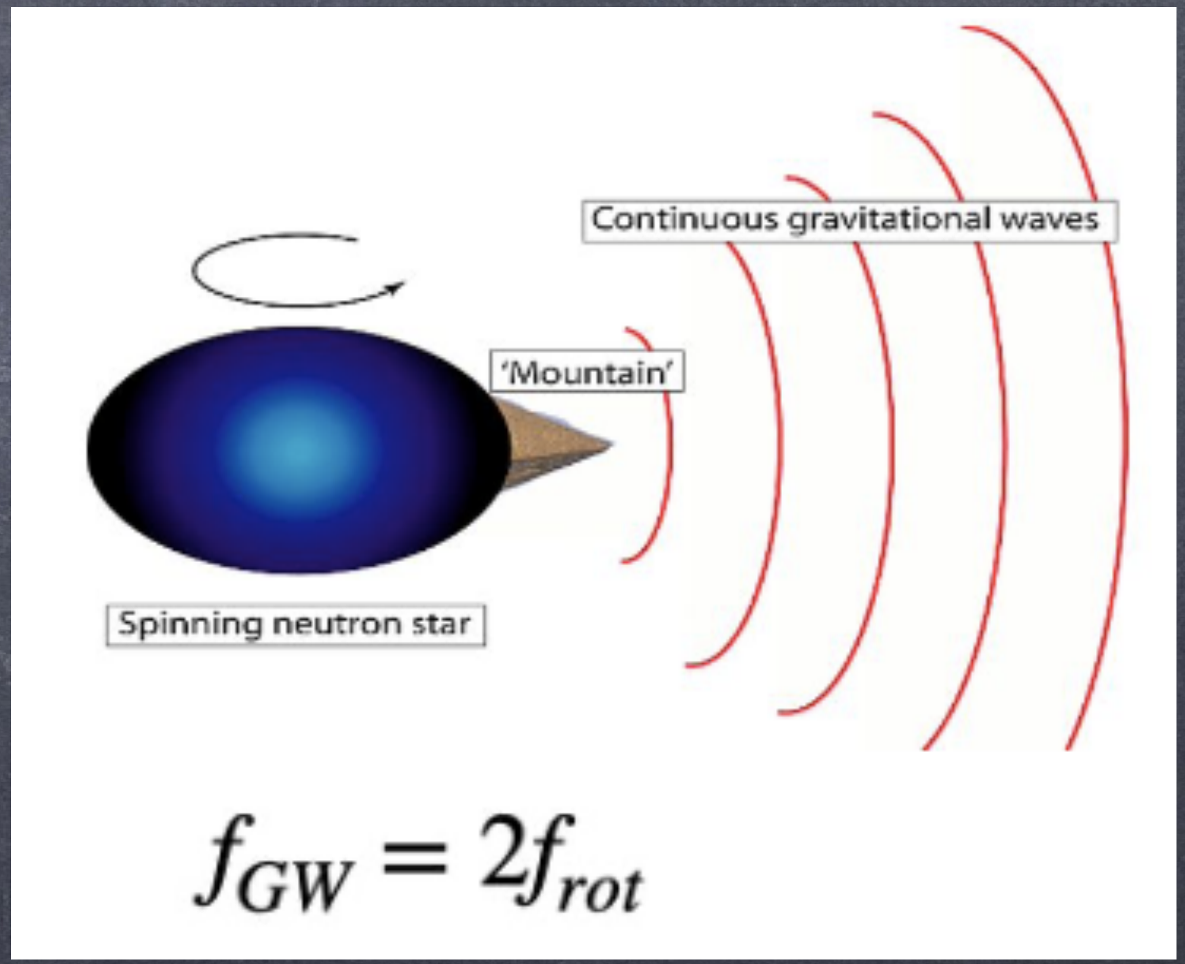

$C_{21} = 0$ and $C_{22} = 2h_0$ where $h_0 = \dfrac{16\pi^2 G}{c^4} \dfrac{I_{zz}\varepsilon f_{\mathrm{rot}}^2}{d}$,

ε is the ellipticity defined as $\varepsilon \equiv \dfrac{|I_{xx} - I_{yy}|}{I_{zz}}$ ε

d is the distance of the source

$$\left(\frac{d}{dt}\left(\frac{1}{2} I_{zz}\Omega^2\right) = \frac{G}{5c^5} < \dddot{Q}_m^{ij}(t')\dddot{Q}_m^{ij}(t') > \right)$$

gives

spin-down limit: $h_0^{\mathrm{sd}} = \dfrac{1}{d}\left(\dfrac{5GI_{zz}}{2c^3} \dfrac{|\dot{f}_{\mathrm{rot}}|}{f_{\mathrm{rot}}}\right)^{1/2}$

A generic metric theory of gravity

Riemann theorem:

No. of DOF in N dimensional metric = $\dfrac{N(N-1)}{2}$

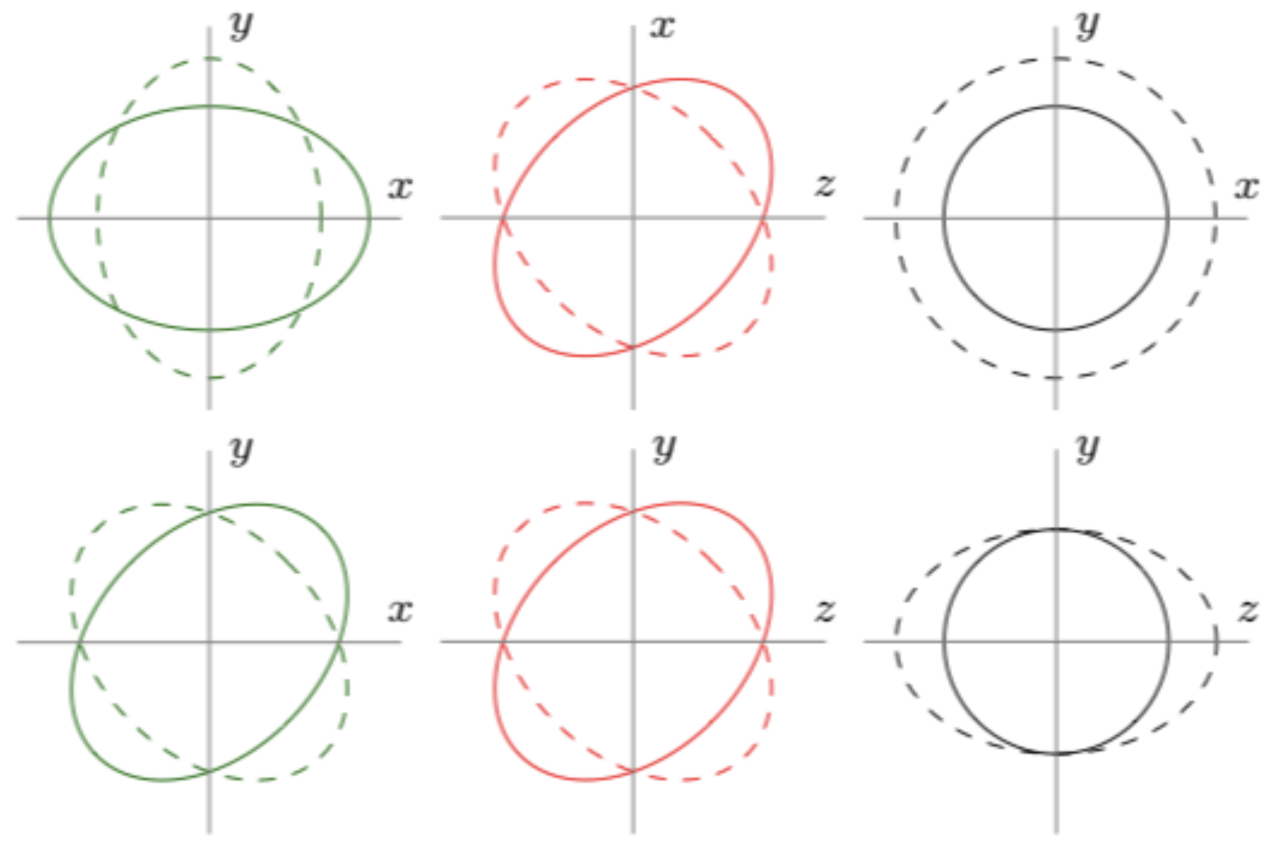

FIG. 1. *Effect of different GW polarizations on a ring of free-falling test particles.* Plus (+) and cross (×) tensor modes (green); vector-x (x) and vector-y (y) modes (red); breathing (b) and longitudinal (l) scalar modes (black). In all of these diagrams the wave propagates in the z direction. This decomposition into polarizations was first proposed for generic metric theories in [7].

Courtesy: LIGO-P1600305

$$\phi = \frac{2\pi}{s}$$

Tensor modes, s = 2
Vector modes, s = 1
Scalar modes, s = 0

gives

4 dimensional metric

Why do we search for non-GR polarizations?

- Hubble tension
- QFT in curved space time

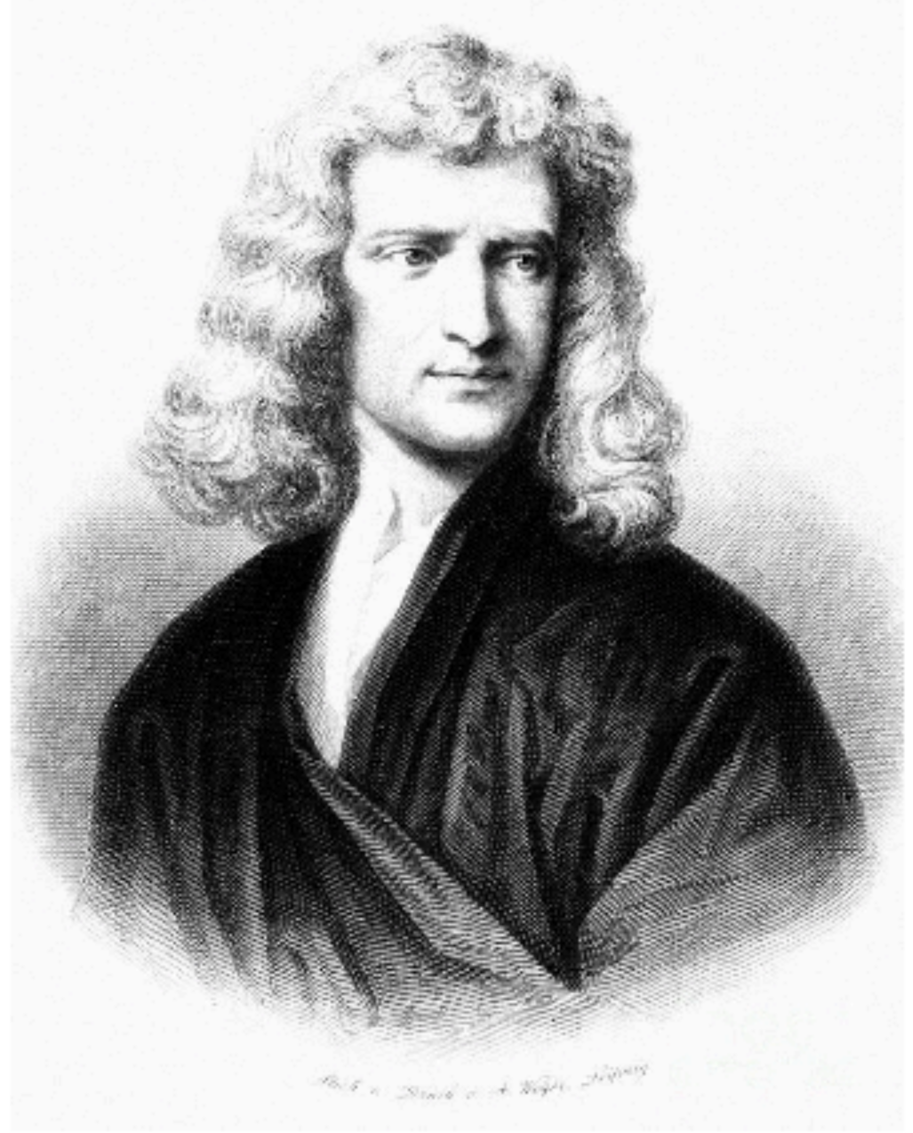

"…there are the ones that invent OCCULT FLUIDS to understand the Laws of Nature. They will come to conclusions, but they now run out into DREAMS and CHIMERAS neglecting the true constitution of things….. …however there are those that from the simplest observation of Nature, they reproduce New Forces (i.e. New Theories)… "

From the Preface of PRINCIPIA (II Edition) 1687 by Isaac Newton, written by Mr. Roger Cotes

Courtesy: S. Capozziello

Dipole radiation in Brans-Dicke (BD) theory

BD theory: 2 tensor states (similar to GR) and 1 scalar state

We assume a spherical star with a tiny mountain on its equator. This mountain can be approximated by a Dirac delta function. In this case: $f_{\rm GW} = f_{\rm rot} \; (l = 1, \, m = 1)$

The signal h_{11} due to the dipole radiation is given by: $h_{11} = -\, h_0^d \, c(\alpha, \delta; t) \, \sin \iota \sin(\Phi(t) + \Phi_0)$

$c(\alpha, \delta; t)$: amplitude modulation function

ζ is the BD parameter obtained observationally

h_0^d : Signal amplitude given by $h_0^d = \dfrac{4\pi G}{c^3} \zeta \dfrac{D f_{\rm rot}}{d}$

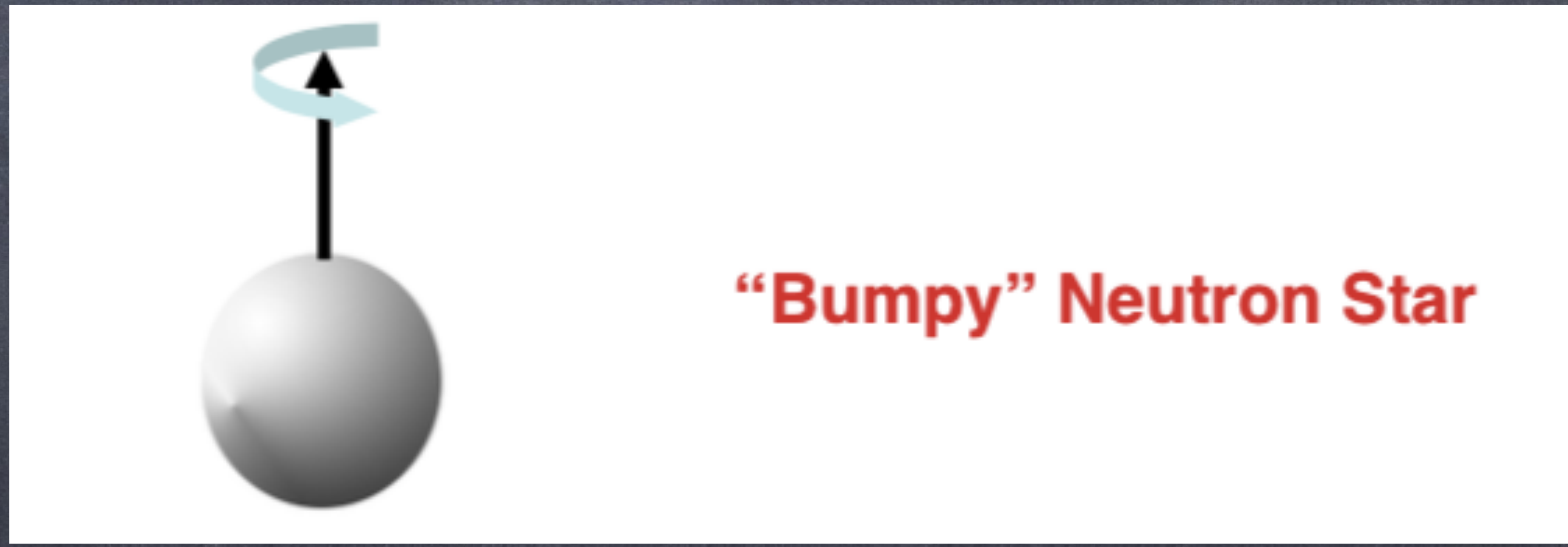

The spin-down limit for the dipole radiation is

$$\frac{d}{dt}\left(\frac{1}{2} I \Omega^2\right) = \frac{c^3}{16\pi G \zeta} \omega^2 r^2 \left(h_0^d\right)^2 < \cos^2(\omega t) > \int_{\iota=0}^{\pi} \int_{\rho=0}^{2\pi} \sin^3 \iota \, d\iota \, d\rho$$

gives

$$h_0^{\rm d,sd} = \frac{1}{d} \left(\zeta \frac{12 G}{c^3} I_{zz} \frac{|\dot{f}_{\rm rot}|}{f_{\rm rot}} \right)^{1/2}$$

(7)

Polarizations

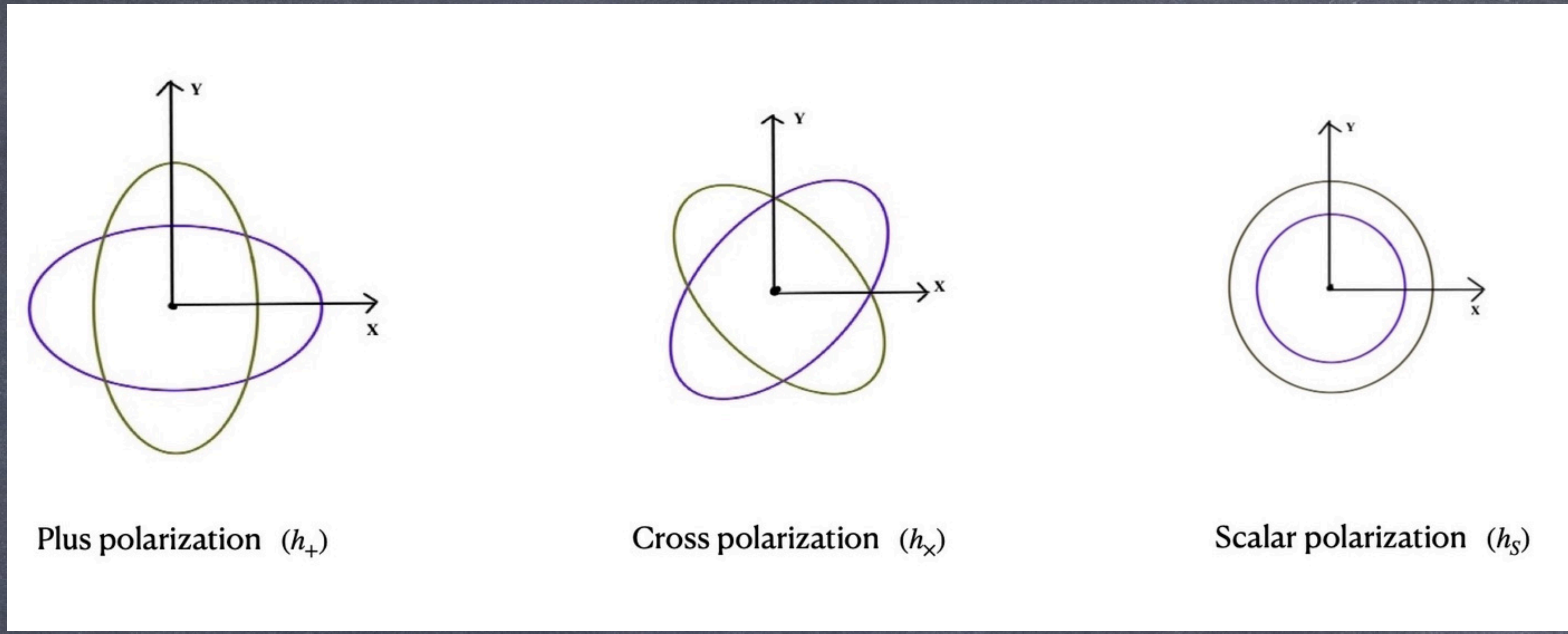

h_+ & $h_\times$:

- Tensor polarizations in GR
- Dominated by time-varying quadrupole moment
- 2-fold symmetric
- Ellipses preserve the area

h_S :

- Scalar polarization in BD
- Dominated by time-varying dipole moment
- ∞-fold symmetric

Data

Electromagnetic data using CHIME, Hobart, Jodrell Bank, MeerKAT, Nancay, NICER and UTMOST observatories.

+

Oct 30, 2016 | O2 | Aug 25, 2017

Virgo (Aug 01, 2017)

+

April 01, 2019 | O3 | March 27, 2020

During O3, the Virgo detector was operational for the entire period.

Search Methods

1. Time domain Bayesian Method

- Fermi Dirac distribution priors on amplitude parameters are used
- Raw GW data is heterodyned using their expected phase evolution
- Includes correction for relative motion of source wrt detectors and various relativistic effects

2. 5n-Vector Method

- Multi-detector matched filter in the frequency domain
- Based on Sidereal modulation of the expected signal amplitude and phase

Search Methods (contd.)

3. $\mathscr{F}/\mathscr{G}/\mathscr{D}$–statistics

unknown

$\mathscr{F}$–statistic: amplitude, phase and polarizations

$\mathscr{G}$–statistic: amplitude & phase polarizations

unknown known

$\mathscr{D}$–statistic: Dipole radiation in BD theory

Analysis

Bayesian analysis	5n-Vector Method	$\mathcal{F}/\mathcal{G}/\mathcal{D}$-statistics
Single Harmonic		Single harmonic
Dual Harmonic	l=2, m=1	Dual Harmonic
		Dipole radiation

Only for 23 high value pulsars

- Total no. of pulsars = 236
- Total no. of pulsars in binaries = 168
- No. of pulsars with $f_{rot} >$ 100 Hz = 161
- No. of high value pulsars ($h_0 < h_0^{sd}$) = 23

Results

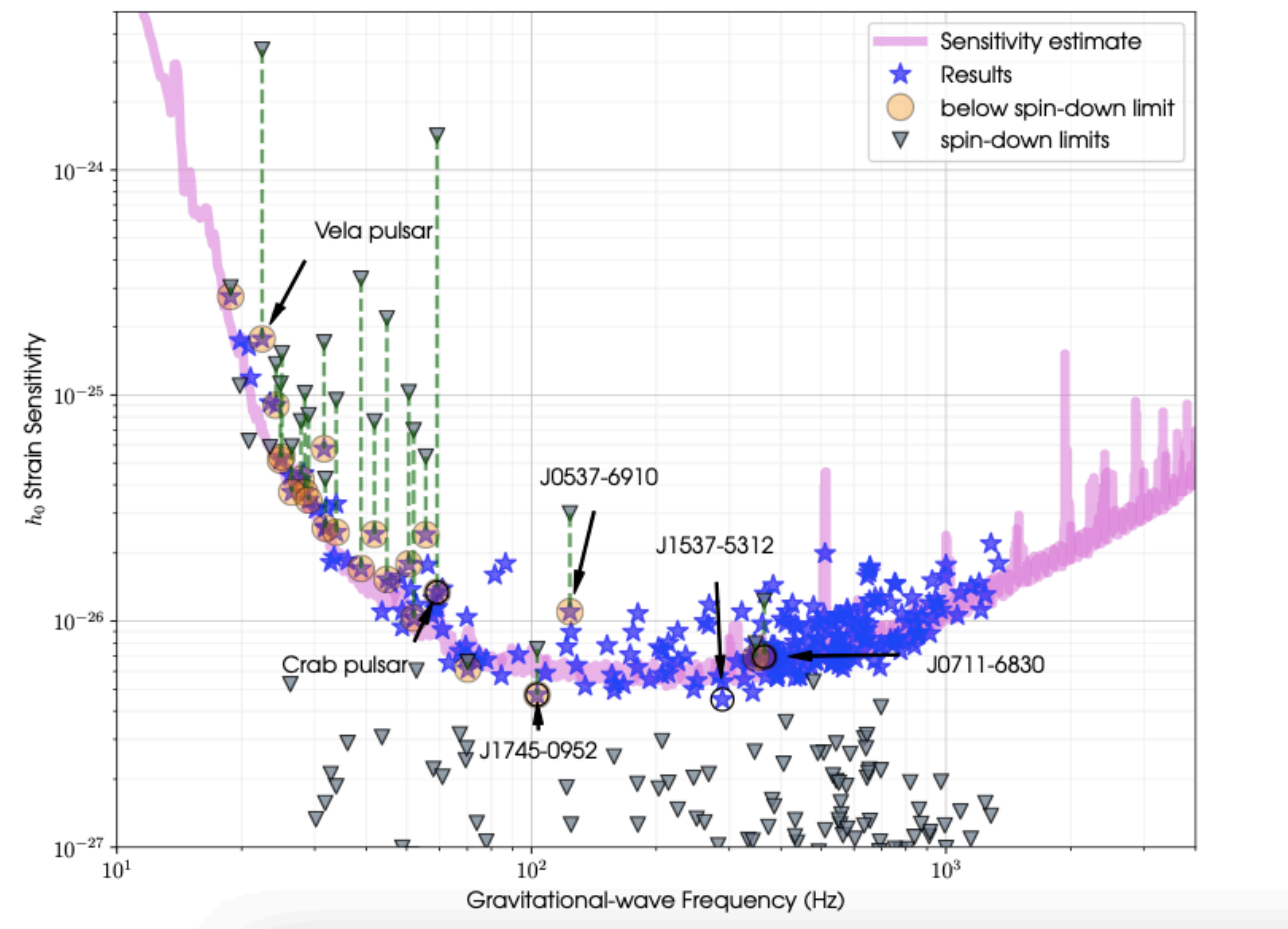

Abbott et al 2022 ApJ 935 1

- Blue stars: 95% credible upper limit for GW amplitude.
- Grey triangle: Spin-down limit for each pulsar
- Shaded circles: h0 for pulsars which surpass the spin-down limits.
- Green dotted line: If upper limit < spin-down limit.
- Solid line: Joint detector sensitivity estimate for O3

$$h_0 \approx 4.23 \times 10^{-26} \left(\frac{1\ \mathrm{kpc}}{\mathrm{d}}\right) \left(\frac{I_{zz}^{fid}}{10^{38}\ \ kg\ m^2}\right) \left(\frac{\epsilon}{10^{-6}}\right) \left(\frac{f_{rot}}{100\ Hz}\right)^2$$

Results (contd.)

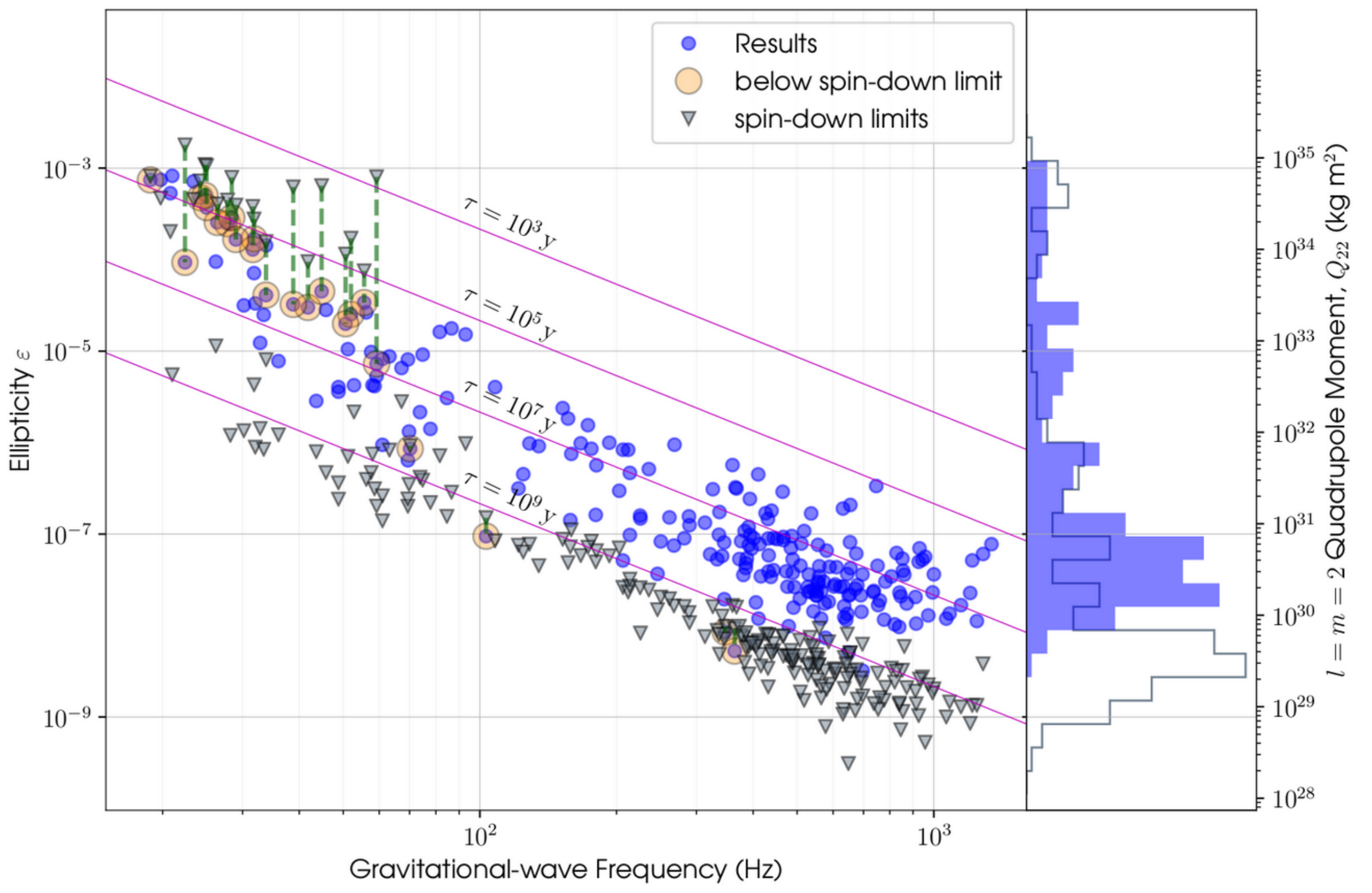

Abbott et al 2022 ApJ 935 1

Limit on mass quadrupole moment which in turn imposes limit on ellipticity.

$$\epsilon \approx 2.36 \times 10^{-6} \left(\frac{h_0}{10^{-25}}\right)\left(\frac{d}{1\ kpc}\right)\left(\frac{100\ Hz}{f_{rot}}\right)^2\left(\frac{10^{38}\ kg\ m^2}{I_{zz}^{fid}}\right)$$

Crab (J0534+2200)	Vela (J0835-4510)
Glitch occurred	No glitch occurred
GWs contributes < 0.009% of the spin-down	GWs contributes < 0.27% of the spin-down
$h_0^{95\%} = 1.3(1.2) \times 10^{-26}$ at d = 2 kpc	$h_0^{95\%} = 1.8(1.7) \times 10^{-25}$ at d = 0.28 kpc
$Q_{22}^{95\%} = 5.6(5.0) \times 10^{32}$ kg-m^2	$Q_{22}^{95\%} = 7.2(7.1) \times 10^{33}$ kg-m^2
$\varepsilon^{95\%} = 7.2(6.5) \times 10^{-6}$	$\varepsilon^{95\%} = 9.3(9.2) \times 10^{-5}$

$h_0^{95\%}$ is the 95% credible upper limits on the amplitudes h_0, $Q_{22}^{95\%}$ is the 95% credible upper limits on the quadrupole moments and $\epsilon^{95\%}$ is the 95% credible upper limits on the ellipticity. Values in parentheses are those produced using the restricted orientation.

Acknowledgement

This material is based upon work supported by NSF's LIGO Laboratory which is a major facility fully funded by the National Science Foundation.

Dziękuję

Bardzo!